Clinical Journal of Gastroenterology (2019) 12:453–459
https://doi.org/10.1007/s12328-019-00951-5

CASE REPORT

Progressive atrophy in a deformed liver as a contributor to sigmoid volvulus

Takahiro Zenda[1] · Ichiro Araki[1] · Naomichi Hamano[1] · Emi Sawada[2] · Otoyuki Nakamiya[2] · Tamao Endo[2] · Hiroto Nishida[2] · Eisuke Ojima[3] · Tatsuo Nakano[3]

Received: 4 January 2019 / Accepted: 14 February 2019 / Published online: 22 February 2019

Abstract
The effect of a prior defect on secondary liver atrophy is unknown. We describe a case of sigmoid volvulus that was facilitated by progressive atrophy in a deformed liver. A 75-year-old man with abdominal pain and fullness was referred to our hospital. Computed tomography (CT) revealed reduced left hepatic lobe volume and a whirl sign, characteristic of sigmoid volvulus. The sigmoid volvulus was successfully detorted with endoscopy. Retrospective evaluation of liver morphology on CT and magnetic resonance imaging showed that the portal vein at the liver hilum was denuded due to a parenchymal defect of the medial segment, with compression by the crossing artery. As pulse Doppler ultrasonography demonstrated reduced portal blood flow in the region where liver atrophy developed, compression of the denuded portal vein presumably facilitated secondary atrophy and contributed to sigmoid volvulus. The present case shows that a deformed liver itself can be a cause of secondary atrophy. Therefore, continued monitoring of liver morphology and evaluation of portal blood flow to predict liver atrophy may be required, when an individual with a partial liver defect is encountered.

Keywords Partial liver defect · Secondary liver atrophy · Denuded portal vein and bile duct · Portal blood flow corrected by perfused liver volume · Sigmoid volvulus

Introduction

Lobular or segmental liver defects are extremely rare [1–9]. Since these are mostly asymptomatic, with normal liver function parameters [1–3, 6], partial defects are usually revealed incidentally during imaging or surgery or at autopsy [5, 8, 9], and rarely in association with complications [1, 4]. Although the features of hepatic defects at the time of diagnosis have been well described in the previous reports [1–10], sequential observation of liver deformities have apparently never been attempted. Herein, we describe a case of progressive atrophy that originated in a large parenchymal defect of the left medial segment (MS) of the liver, leading to a sigmoid volvulus. A possible pathogenic linkage between antecedent liver deformity and subsequent liver atrophy is also discussed.

Case report

A 75-year-old Japanese man was referred to our hospital with a 2-day history of left lower abdominal pain and upper abdominal distention. The patient had a past medical history of cerebral infarction with left incomplete hemiplegia at the age of 53, epididymitis, endoscopic submucosal dissection for the early stage gastric cancer, laparoscopic cholecystectomy for acute calculous cholecystitis at the age of 68 in 2010, total hip arthroplasty for coxarthrosis at the age of 69, and endoscopic choledocholithotomy for acute cholangitis at the age of 72 in 2013. The patient did not consume alcohol or smoke.

At presentation, the patient's general condition was good, with stable vital signs: body temperature 36.8 °C, blood pressure 141/88 mmHg, pulse rate 88 beats/min, and

✉ Takahiro Zenda
zenda@asanogawa-gh.or.jp

[1] Department of Internal Medicine, Asanogawa General Hospital, Kosaka-machi Naka 83, Kanazawa 920-8621, Japan

[2] Department of Radiology, Asanogawa General Hospital, Kanazawa, Japan

[3] Department of Surgery, Asanogawa General Hospital, Kanazawa, Japan

peripheral arterial oxygen saturation 96%. Other than mild left hemiplegia, examination revealed asymmetrical upper abdominal bulging with severe distension, and tenderness in the left lower abdomen. Plain abdominal radiography revealed a semi-looped and disproportionately enlarged sigmoid colon (Fig. 1). Plain chest radiography revealed large intestinal gas shadows beneath the bilateral diaphragm. On the right, interposition of gas shadows between the diaphragm and liver represented Chilaiditi's sign [11, 12] (Fig. 2). Computed tomography (CT) with contrast revealed a soft-tissue mass with swirling of the intestinal wall, vessels, and mesenteric adipose tissue, i.e., a whirl sign characteristic of intestinal volvulus [13] (Fig. 3a arrow), consistent with the location of tenderness. The mesenteric artery in the soft-tissue mass was clearly enhanced by contrast medium, but edematous colonic wall thickening and ascites were not evident (Fig. 3a). CT concomitantly revealed a defect of the left lobe of the liver. The grossly dilated large intestine was interposed between the liver and diaphragm or abdominal wall (Fig. 3b). The peripheral blood cell count and inflammatory markers showed no abnormalities. Liver function test results were almost normal (reference ranges in parentheses): alanine aminotransferase, 18 IU/L (13–33 IU/L); aspartate aminotransferase, 7 IU/L (8–42 IU/L); alkaline phosphatase, 312 IU/L (115–359 IU/L); gamma-glutamyl transpeptidase, 19 IU/L (10–47 IU/L); total bilirubin, 1.3 mg/dL (0.4–1.2 mg/dL); serum albumin, 3.9 g/dL (4.0–5.0 g/dL); and prothrombin time, 72.2% (70–130%). Viral markers were negative for hepatitis B surface antigen and hepatitis C virus antibody. Negative results for serum Mac-2-binding protein glycosylation isomer and normal shear wave velocity of 1.3 m/s suggested that hepatic fibrosis associated with chronic liver disease was unlikely.

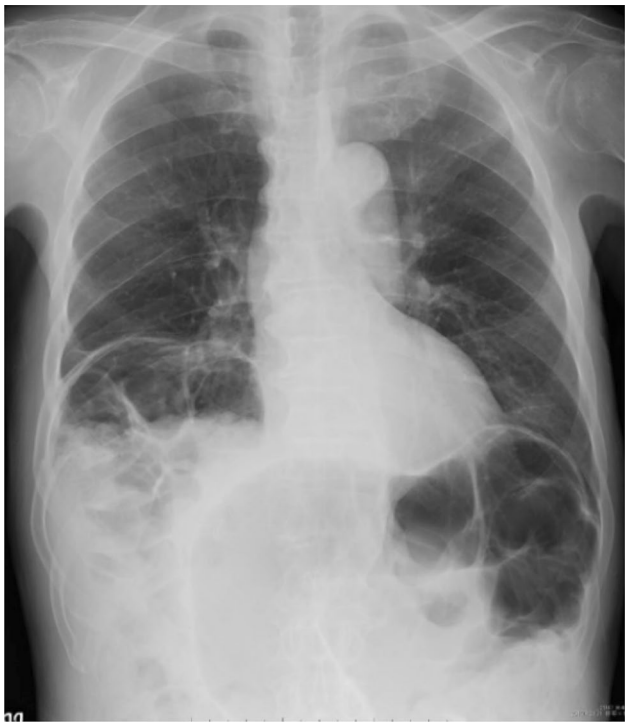

Fig. 2 Plain chest X-ray showed an elevated right hemidiaphragm. Looped colonic gas shadows were found bilaterally beneath the diaphragm. Hepatodiaphragmatic interposition of the large intestine represents Chilaiditi's sign

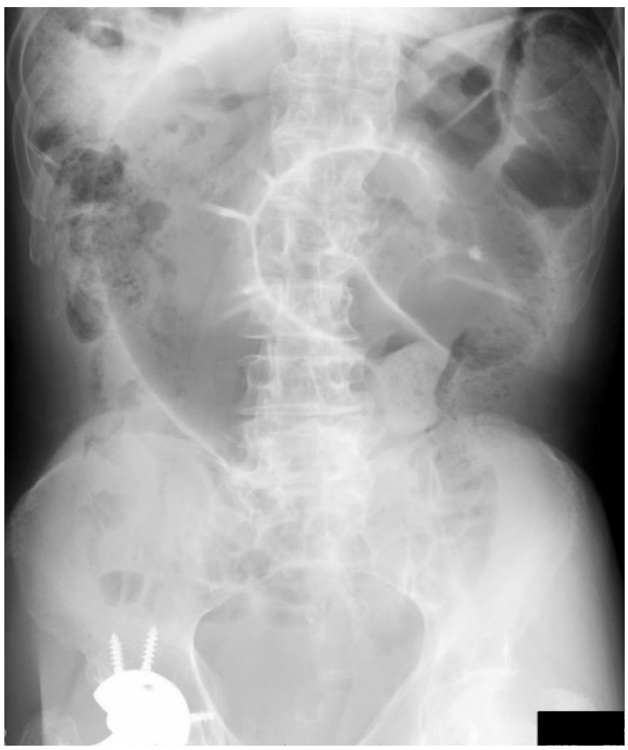

Fig. 1 Plain abdominal X-ray showed a sigmoid colon that was grossly dilated by air and semi-looped

The patient was considered to have a sigmoid volvulus with reduced mesenteric blood flow based on the enhanced CT findings and physical examination, and emergent endoscopic detorsion was attempted. Emergent endoscopy showed that the colonic mucosa was intact, and the intestinal lumen showed spiral obstruction at 23 cm from the anal verge. The sigmoid volvulus was successfully detorted with endoscopy and the abdominal symptoms subsided dramatically. The patient underwent prophylactic selective sigmoidectomy 1 month later because of the expected high risk of recurrence of volvulus due to a long loop of redundant sigmoid colon and the large parenchymal liver defect. The smooth surface and sharp liver edge observed during surgery appeared normal (Fig. 4). The postoperative course was uneventful.

We retrospectively reevaluated the deformity of the left hepatic lobe based on previous CT and magnetic resonance imaging (MRI). When the patient underwent laparoscopic

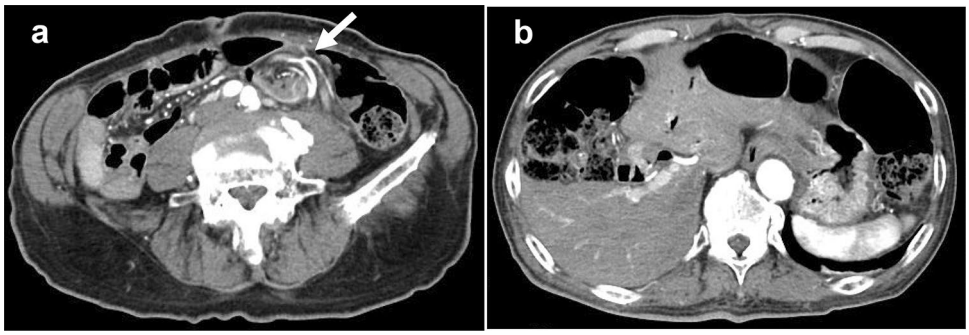

Fig. 3 Computed tomography (CT) with contrast medium. The slice at the location of abdominal tenderness showed a soft-tissue mass consisting of swirling intestinal wall, vessels, and mesenteric adipose tissue, i.e., whirl sign (**a**: arrow), which was highly suggestive of intestinal volvulus. The mesenteric artery is clearly enhanced by contrast medium in the soft-tissue mass. Neither edematous intestinal wall thickening nor ascites were evident around the soft-tissue mass (**a**). CT concomitantly disclosed gross volume reduction of the left hepatic lobe and hepatodiaphragmatic interposition of the large intestine dilated with air (**b**)

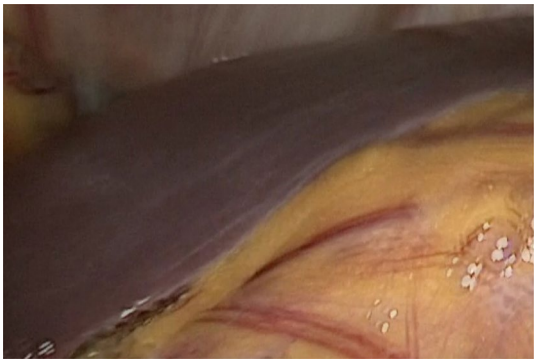

Fig. 4 Appearance of the liver during sigmoidectomy. The liver surface and edge appeared normal

cholecystectomy in 2010, a marked defect of the MS was evident (Fig. 5a, b). The bilateral hepatic lobes were only connected through a narrow isthmus, which predominantly consisted of the caudate lobe and included the liver hilum. The portal vein, hepatic artery, and bile duct were entirely denuded along the isthmus (Fig. 5b), and the inflamed gallbladder was located adjacent to these structures (Fig. 5a, b). Between 2010 and 2018, sequential CT or MRI apparently showed the atrophy of the lateral segment (LS) of the liver (Fig. 5a–e). Analysis using the Ziostation 2 PLUS software (Ziosoft Co. Ltd., Tokyo) demonstrated marked volume reduction in the left lobe, predominantly consisting of the LS and caudate lobe, from 323 to 155 cm^3 (48.0%) over a period of 7 years, although atrophy of the right lobe was also apparent (Table 1). However, despite the large parenchymal defect of the MS, branches of the bile duct, hepatic artery, and portal vein were identifiable on magnetic resonance cholangiography (Fig. 6) or CT angiography (Fig. 7). Of note, the left portal vein branch appeared to be compressed backward by the crossing left hepatic artery, causing the LS portal branches to become tapered (Fig. 7). The portal blood flow volume per unit of perfused liver volume, estimated with pulse Doppler ultrasonography in 2018 (Fig. 8), was actually much decreased in the left portal vein at the umbilical portion compared to that in the right portal vein, measuring 0.35 and 0.90 mL/min/cm^3 of liver, respectively (Table 2). The patient remains carefully monitored for progression of liver atrophy.

Discussion

As Merrill reported only 1 case (0.005%) out of 19,000 autopsy cases [8], congenital partial defects of the liver have been considered rare [1–7, 9]. Unless a hepatic defect affects surrounding organs, the condition may remain mostly asymptomatic, with normal liver function test results [1–3, 6, 7]. A partial liver defect is noted incidentally during surgery or autopsy [5, 9] or in association with complications such as cholelithiasis [4], hepatic neoplasia [1], Chilaiditi's syndrome [2, 11], gastric ulcer [1, 4], or volvulus of the stomach [4] or sigmoid colon [1] as in the present case.

Hepatic defects are either congenital or acquired [1, 2, 4, 6, 9]. Ormeci et al. emphasized the need for differentiation between agenesis (absence of a lobe, with replacement by fibrous tissue), aplasia (development of a small lobe, with abnormal hepatic trabeculae, bile ducts, and blood vessels), and hypoplasia (development of a small lobe with normal tissue structures), based on the intrahepatic structure of the biliary system and vessels [3]. The presumed mechanisms of these congenital hepatic anomalies include dysgenesis of the hepatic primordium during the early specific embryonic stage [2, 4, 5], umbilical vein anomalies [1, 5, 6], immature development of the portal vein with thrombotic occlusion [1, 5, 9], impairment of the nutritional supply via the hepatic cord [5], and minor positional anomalies of the other organs that interfere with growth of the hepatic parenchyma

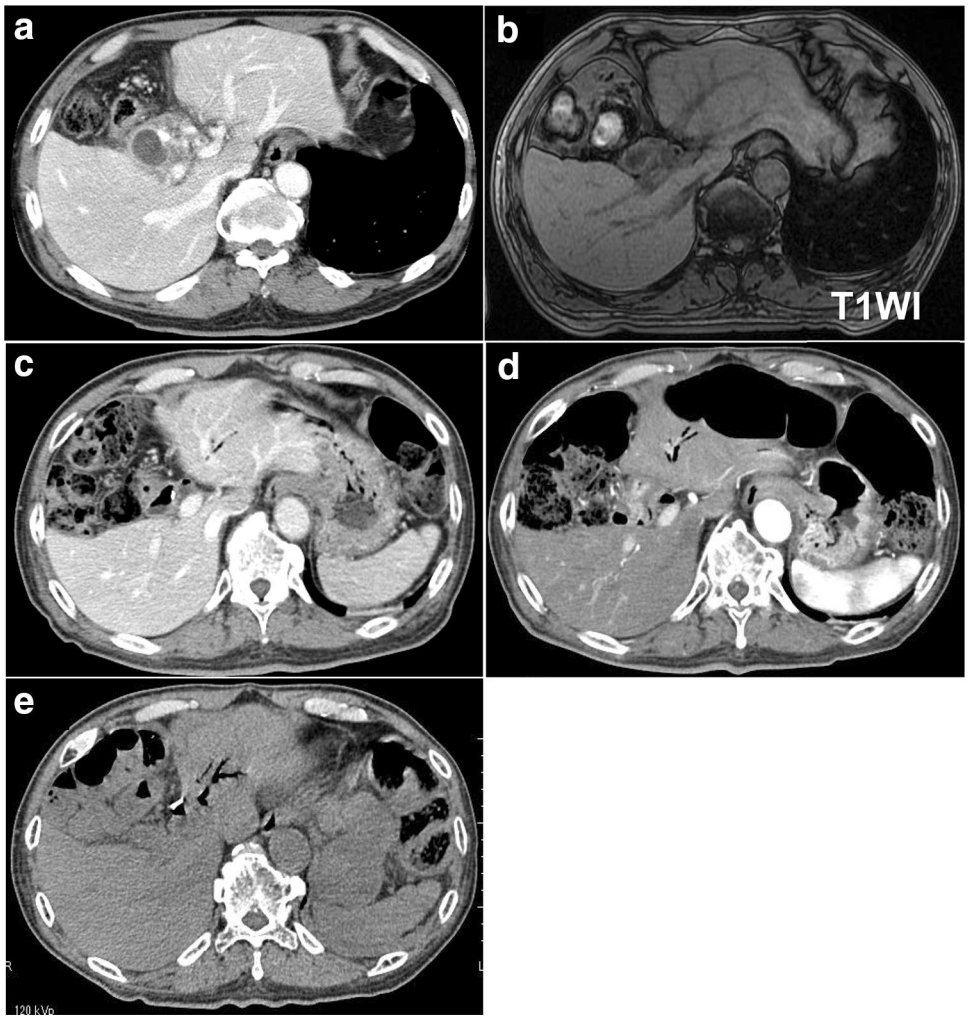

Fig. 5 Sequential morphologic changes in the liver on computed tomography (CT) and magnetic resonance imaging (MRI). When the patient underwent laparoscopic cholecystectomy for acute calculous cholecystitis in 2010, a marked defect of the medial segment (MS) of the liver was already evident (**a, b**). Due to the parenchymal defect, the bilateral hepatic lobes were connected only through the narrow isthmus, which predominantly consisted of the caudate lobe and included the liver hilum (**b**). The portal vein, hepatic artery, and bile duct were entirely denuded along the isthmus (**b**), where the inflamed gallbladder was located (**a**). Sequential CT and MRI imaging (**a–e**) between 2010 and 2018 shows progressive atrophy of the lateral segment (LS) of the liver. Due to the expanded large intestine in association with sigmoid volvulus, the LS was considerably depressed (**d**). LS depression disappeared after sigmoidectomy (**e**). **a** CT with contrast in 2010, **b** plain MRI with T1-weighted imaging (T1WI) in 2010, **c** CT with contrast in 2015, **d** CT with contrast in 2017, **e** plain CT in 2018

Table 1 Sequential change in liver volume

Year. Month	2010. 5	2014.12	2015.9	2017.10
S1–S4 (left lobe) (cm^2)	323	260	172	155
S5–S8 (right lobe) (cm^2)	1170	1012	743	769
S1–S8 (total liver) (cm^2)	1493	1272	915	924
S1–S4/S1–S8 (cm^2)	21.6	20.4	18.7	16.8

Segment (S) 1–S4 and S5–S8 represent the left and right hepatic lobes, respectively. In the present case, S1–S4 principally consisted of the caudate lobe and lateral segment. Although the total liver volume (S1–S8) was decreased to 61.9%, volume reduction of the left lobe (S1–S4) was the greatest at 48% (from 323 to 155 cm^3) during the 7 years from 2010 to 2017

[5]. On the other hand, liver atrophy is usually defined as an acquired tissue volume loss of at least 50% [10] and is caused by secondary vascular and biliary flow disturbances, neoplasms, cirrhosis, severe malnutrition, or prior surgery or trauma, among others [1–4, 9, 14]; of these, cholangiocarcinoma arising at the liver hilum and post-cholecystectomy stricture are the most common causes reported [2, 10].

In the present case, the MS was present but very small, because branches of the hepatic artery, portal vein, and bile duct corresponding to the MS could be definitely identified on either CT angiography (Fig. 7) or MR cholangiography (Fig. 6). No apparent cause of MS atrophy was identified. Although differentiation between congenital hypoplasia and atrophy of the liver is critical but often difficult [1, 4, 6, 9], an antecedent parenchymal MS defect in this case was more likely due to hypoplasia than atrophy, similar to a documented case of hepatic hypoplasia in which the main vessels were present despite the complete absence of parenchyma [5]. On the other hand, sequential LS observation on CT and MRI (Fig. 5a–e) documented the progressive parenchymal volume reduction of more than 50%, i.e., secondary atrophy. Although features of partial liver defects at the time of diagnosis have been well documented [1–10], we have shown that secondary atrophy occurs in a liver with partial parenchymal defects.

In the present case, we speculate that LS atrophy may have been associated with an antecedent parenchymal MS defect (Fig. 9). Owing to this marked defect, the right lobe

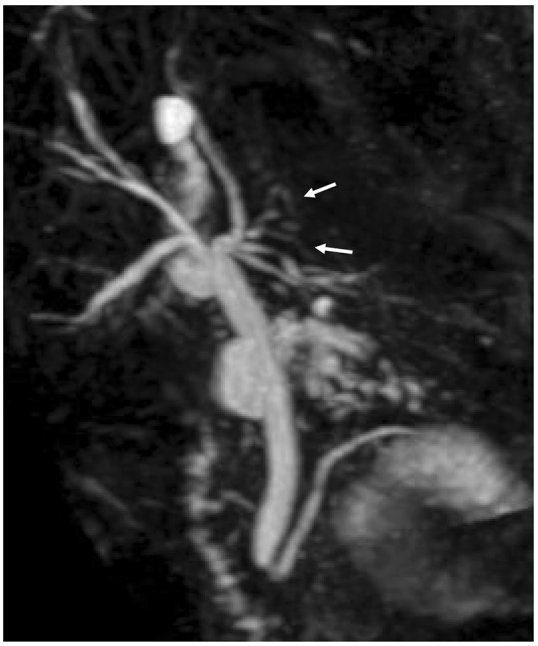

Fig. 6 Magnetic resonance cholangiography in 2010. Bile duct branches corresponding to the left medial segment (MS) of the liver are identifiable (arrows), despite a severe parenchymal defect of the MS

and LS were connected only through the isthmus, possibly corresponding to a previously described "bipartite liver" [7]. This isthmus predominantly consisted of the caudate lobe and included a crucial location of the liver hilum [2]. Due to the parenchymal loss, the portal vein, hepatic artery, and bile duct were entirely exposed to the exterior of the isthmus. Moreover, the parenchymal defect diminished the gallbladder fossa [9] leading to an anomalous position and hypermobility [1, 6, 9], as the inflamed gallbladder was located adjacent to the exposed portal vein and bile duct in the liver hilum (Fig. 5a).

Under such conditions, it is plausible that the exposed portal vein and bile duct had been compressed by the hepatic artery, malpositioned gallbladder, or intestine intruding on the vacant MS space [2], intermittently affected by increased intraabdominal pressure during daily life or twisted due to the fragile isthmus [7]. Compared with the artery, the portal vein and bile duct are more easily crushed because of low wall resistance to external pressure. Indeed, we demonstrated with pulse Doppler ultrasonography that blood flow in the left portal vein branch was markedly decreased compared to that in the right branch; this was in agreement with the CT angiography findings that the crossing left hepatic artery directly compressed the left portal vein, causing the LS portal branches to become thinner. Chronic flow disturbance in the portal vein is reportedly more problematic than that in the bile duct [2, 14], and might have facilitated progressive LS atrophy. In addition, considering that the LS atrophy rapidly developed after acute calculous cholecystitis and cholecystectomy, some inflammatory or surgical influence on the portal vein and bile duct around the liver hilum could not be excluded [14] (Fig. 9).

Blood flow volume in the truncal portal vein measured directly during cholecystectomy in 8 patients was 704.0 ± 230.9 mL/min [15], or 869.4 ± 184.0 mL/min when measured with pulse Doppler ultrasonography in 60 healthy subjects [16]. Yamauchi et al. proposed using the ratio of truncal portal blood flow volume to the total liver volume measured with MRI in 43 subjects, including 8 healthy volunteers, 13 patients with chronic hepatitis, and 22 patients with cirrhosis, to calculate respective index values of

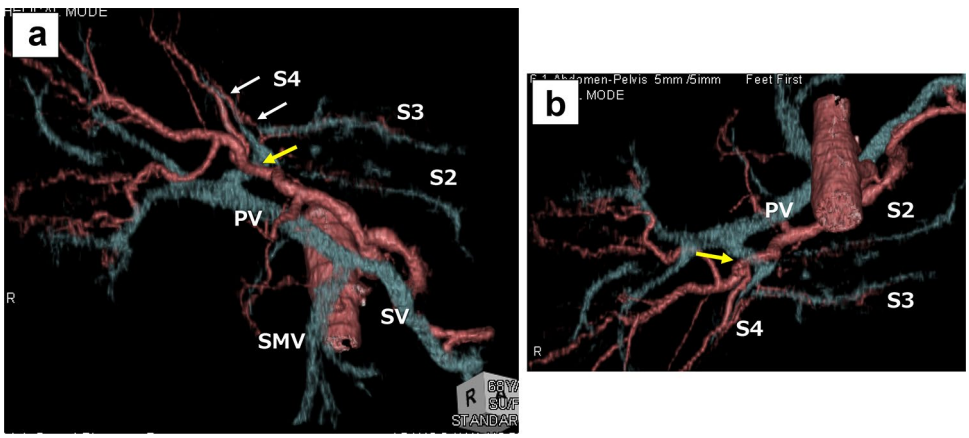

Fig. 7 Three-dimensional reconstructed computed tomographic angiography in 2010. Arterial and portal vein branches corresponding to the middle hepatic segment were identifiable (white arrows). The left arm of the portal vein appeared compressed backward by the crossing left hepatic artery (yellow arrow), and the LS portal branches became thinner. **a** View from lower ventral site and **b** view from upper dorsal site. Blue and pink vessels represent the portal vein and artery, respectively. *S* segment, *PV* portal vein, *SV* splenic vein, *SMV* superior mesenteric vein

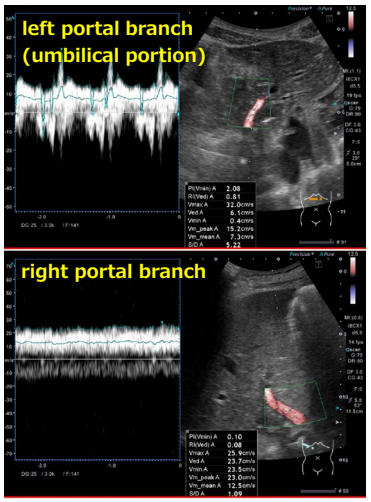

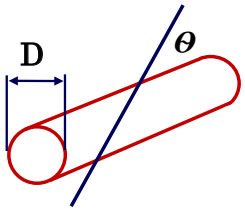

$$\text{PBF}_{(\text{ml/min})} = \frac{D \times D \times \pi}{4} \times \frac{V_{mean}}{\cos\theta} \times 60$$

PBF: portal vein blood flow

D: diameter

θ: incident angle between the Doppler beam and the portal vein

V_{mean}: mean velocity

Fig. 8 Evaluation of portal vein flow with pulse Doppler ultrasonography. After measuring the mean blood flow velocity of bilateral portal vein branches with pulse Doppler ultrasonography, each flow volume was calculated according to a formula, assuming that the cross section of the portal vein was completely round. In turn, each portal blood flow volume was corrected by the liver perfusion volume

Table 2 Portal vein flow volume

	Diameter (cm)	Mean velocity (cm/min)	Blood flow volume (*a*) (ml/min)	Perfused liver volume (*b*) (cm^2)	Blood flow per unit liver volume (*a*/*b*) (ml/min/cm^3 of liver)
Left portal branch (umbilical portion)	0.38	7.3	56.8	155	0.35
Right portal branch	0.85	12.5	691.0	769	0.90
Total liver	–	–	747.8	924	0.81

Portal blood flow per unit of perfused liver volume was apparently decreased in the left portal vein at the umbilical portion compared to that in the right portal vein, measuring 0.35 and 0.90 mL/min/cm^3 of liver, respectively

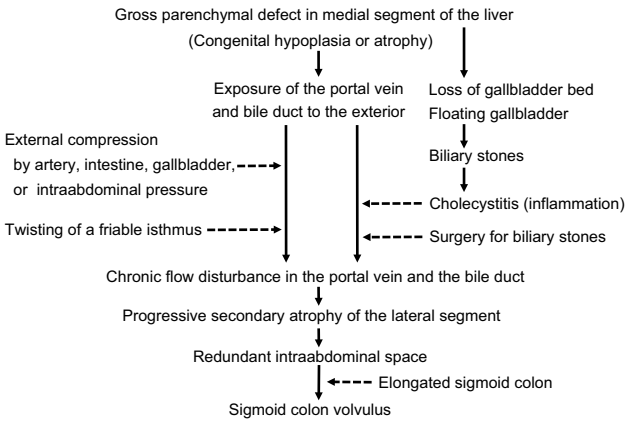

Fig. 9 Possible pathophysiology in the present case

0.8 ± 0.1, 0.7 ± 0.2, and 0.6 ± 0.4 mL/min/cm^3 of liver [17]. They also showed that this index correlated well with liver volume, except in patients with cirrhosis [17]. In the present case, total portal flow volume (747.8 mL/min) and the corrected flow volume in the right portal branch (0.90 mL/min/cm^3 of liver) were compatible with the reported standard values, but the corrected flow volume in the left portal branch (0.35 mL/min/cm^3 of live) was apparently decreased (Table 2). These results suggest that evaluation of lobular or segmental portal flow volume corrected by perfused liver volume may be useful for predicting liver atrophy in an individual with a partial liver defect or following hepatobiliary surgery. Furthermore, MRI with contrast may be useful for calculating such an index, because it can measure both portal flow volume and liver volume concurrently [17].

As LS volume reduction is closely associated with the occurrence of sigmoid volvulus [18], it is possible that progressive LS atrophy concurrent with the antecedent MS parenchymal defect provided redundant space in the abdominal cavity, into which the large intestine intruded to form hepatodiaphragmatic interposition. This elderly man's risk factors included a history of cerebral infarction and an elongated sigmoid colon [11, 12], leading to the rare condition of sigmoid volvulus with Chilaiditi's sign [12] (Fig. 9).

In summary, this case demonstrated that a liver defect not only caused acute abdominal distress from a sigmoid volvulus, but also promoted secondary liver atrophy, probably through impairment of flow in the portal vein and/or biliary system. It is, thus, necessary to monitor the possible development of delayed atrophy [14] or to evaluate portal blood

flow for the prediction of atrophy, when an individual with a partial liver defect including the liver hilum is encountered.

Acknowledgements The authors are particularly grateful to Kei Hamazaki, (Assistant Professor, Department of Public Health, Faculty of Medicine, University of Toyama) for his document retrieval and constructive comments and criticisms.

Compliance with ethical standards

Conflict of interest None of the authors have received any grant associated with this case report. All authors declare that they have no conflict of interest.

Human rights All procedures followed have been performed in accordance with the ethical standards laid down in the 1964 Declaration of Helsinki and its later amendments.

Informed consent Informed consent was obtained from the patient for being reported in this journal.

References

1. Matsushita K, Gotoh K, Eguchi H, et al. Agenesis of the left hepatic lobe undergoing laparoscopic hepatectomy for hepatocellular carcinoma: a case report. Surg Case Rep. 2017;3:50. https://doi.org/10.1186/s40792-017-0325-z.
2. Ceravolo I, Guerrieri D, De Vargas Macciucca M, et al. MRI rare finding: absence of the left liver lobe. Eur J Radiol Open. 2017;4:50–2.
3. Ormeci T, Erdogan ST, Ormeci A, et al. A rare congenital liver anomaly: hypoplasia of left hepatic lobe. J Pak Med Assoc. 2016;66:1662–4.
4. Koh H, Lee JS, Park YJ, et al. Gastric volvulus associated with agenesis of the left lobe of the liver in a child: a case treated by laparoscopic gastropexy. J Pediatr Surg. 2008;43:231–3.
5. Saigusa K, Aoki Y, Horiguchi M. Hypoplasia of the left lobe of the liver. Surg Radiol Anat. 2001;23:345–7.
6. Maeda N, Horie Y, Shiota G, et al. Hypoplasia of the left hepatic lobe associated with floating gallbladder: a case report. Hepatogastroenterology. 1998;45:1100–3.
7. Burton BE, Amin EA, Tisdale P. Bipartite liver. A case report. Clin Nucl Med. 1987;12:641–3.
8. Merrill GG. Complete absence of the left lobe of the liver. Arch Pathol (Chic). 1946;42:232–3.
9. Kakitsubata Y, Nakamura R, Mitsuo H, et al. Absence of the left lobe of the liver: US and CT appearance. Gastrointest Radiol. 1991;16:323–5.
10. Friesen BR, Gibson RN, Speer T, et al. Lobar and segmental liver atrophy associated with hilar cholangiocarcinoma and the impact of hilar biliary anatomical variants: a pictorial essay. Insights Imaging. 2011;2:525–31.
11. Chen S, Liu C, Tsai Y, et al. Sigmoid volvulus and associated Chilaiditi's syndrome. Rev Esp Enferm Dig. 2007;99:482–3.
12. Lucas Ramos J, Poza Cordon J, Froilán Torres C, et al. Chilaiditi syndrome complicated by a sigmoid volvulus and hepatic displacement. Rev Esp Enferm Dig. 2017;110. https://doi.org/10.17235/reed.2017.5197/2017.
13. Shaw WZ, Huang CF, Hung TY, et al. Typical whirl sign in sigmoid volvulus. J Emerg Med. 2014;46:383–4.
14. Ishida H, Naganuma H, Konno K, et al. Lobar atrophy of the liver. Abdom Imaging. 1998;23:150–3.
15. Schenk WG Jr, McDonald JC, McDonald K, et al. Direct measurement of hepatic blood flow in surgical patients: with related observations on hepatic flow dynamics in experimental animals. Ann Surg. 1962;156:463–71.
16. Sato S, Tsubaki T, Kako M, et al. Measurement of portal and splenic venous flow volume (PV and SV), congestion index (CI) and SV/PV% in various liver diseases using by Doppler echosonography. (In Japanese abstract in English) Nihon Shokakibyo Gakkai Zasshi. 1996;93:331–7.
17. Yamauchi A, Honda N, Kawamoto C, et al. Portal blood flow in chronic liver disease: measurement of portal blood flow using 2D-cine phase contrast magnetic resonance angiography. (In Japanese abstract in English) J Saitama Medical University. 2011;37:103–12.
18. Barral M, Lassalle L, Dautry R, et al. Volvulus of the sigmoid colon is associated with hypotrophy of the left lateral segment of the liver and the absence of sigmoid diverticulum. Diagn Interv Imaging. 2018;99:247–53.